14th Australasian Fluid Mechanics Conference
Adelaide University, Adelaide, Australia
10-14 December 2001

Optically Addressed Pressure Sensors for Transient Gas Dynamics: Calibration of a Preliminary Design

S.A. Sharifian and D.R. Buttsworth

Faculty of Engineering and Surveying
University of Southern Queensland, Toowoomba, 4350 AUSTRALIA

Abstract

The design of pressure sensors based on interferometric measurements of diaphragm deflection for transient gas dynamics experiments is discussed. Quasi-steady calibration results from one such sensor are presented. Results from a dynamic calibration of the same sensor are also described. Predictions of diaphragm behaviour based on a clamped circular diaphragm model are within about 30% of the results obtained from the static and dynamic calibrations. However, a strong temperature sensitivity is also apparent. Future development will focus on reducing the temperature sensitivity of the sensor in transient applications.

Introduction

Pressure is a fundamental parameter that needs to be measured in virtually all gas dynamics experiments. A wide variety of commercial piezoelectric and piezoresistive pressure sensors are currently available. The installation of these sensors in protective static and pitot pressure measurement configurations allows measurements to a bandwidth of a few kHz. However, accurate measurements of higher frequency pressure fluctuations during transient gas dynamics experiments are also of interest, and for this work, fast-response devices with a useful bandwidth to at least 100kHz are required. While such bandwidths can be achieved using commercial devices, the cost of the experiments can become prohibitive.

For example, response times of between 1 and 2 μs are typically quoted for the commercial piezoelectric pressure transducers typically used in shock tunnel flows. But the harsh and often particle-contaminated flow environment coupled with the relatively high transducer cost (in excess of $1000 Australian) generally makes it necessary to avoid exposing the diaphragm directly to the flow. Shielding these commercial transducers with protective material on their diaphragm or by mounting them within a protective pneumatic cavity can reduce the effective measurement bandwidth and render them unsuitable for unsteady pressure measurements in shock tunnel environments. Fluctuation measurements have previously been reported using a cavity-protected transducer arrangement [3], but the resonant frequency of the cavity is estimated at around 10kHz, so the maximum useful bandwidth would be around 3kHz only.

Cost-effective fast-response pressure measurements can be obtained in shock tube and expansion tube flows using 'bar gauges' constructed in-house [6,7]. The bar gauge design consists of a piezoelectric film sandwiched within or cemented around the circumference of a cylindrical bar. The bar has one of its circular ends exposed to the oncoming flow for the measurement of pitot pressure. Bar gauges must be calibrated dynamically as they produce no steady state output. The measurement rise-time depends on the length of the piezoelectric film in the axial direction of the bar, and the strain wave speed within the bar. Depending on the design, the measurement rise time can be less than 1μs. The diameter of the bar and hence the spatial resolution of the devices is usually around 2mm.

Equally cost-effective and fast-response pressure measurement devices can be designed using fibre optic technology [4,5]. These devices measure the pressure-induced displacement of a small diaphragm using a fibre-optic interferometer system. The principal advantages of the optical measurement system over the bar gauges are: 1) a steady state pressure response is provided by the optical system; and 2) the optical system has a spatial resolution around an order of magnitude higher than the bar gauges.

Transducer Arrangement

Optical System

The interferometer system used in the current work is illustrated in figure 1. Light from a 20mW laser diode at 780nm is launched into a single mode fibre attached to a 50/50 bi-directional coupler. Light reflects off the cleaved end of the fibre which is located about 15μm from the diaphragm and propagates back towards the signal detector. Light transmitted into the air cavity reflects off the diaphragm and this light also propagates back towards the signal detector. Deflection of the diaphragm due to changes in the external pressure alters the length of the air cavity and thus the relative phase of the two reflected signals. Changes in the relative phase of the two reflected waves are identified as changes in the intensity at the signal detector.

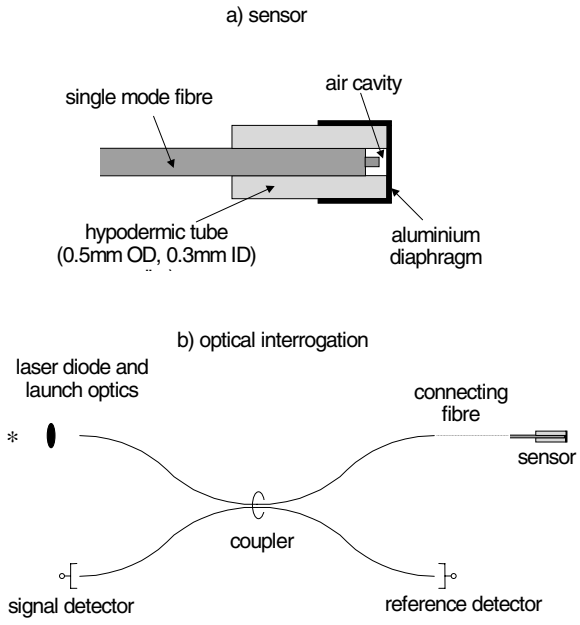

Figure 1. Pressure transducer arrangement.

Sensor Construction

Details of the sensor arrangement are presented in figure 1. Aluminium foil (supermarket quality) is pretensioned and cemented onto the end of a hypodermic tube (25G x 1½'' – outside diameter of about 0.5mm, inside diameter of about 0.3mm) using cyanoacrylate. Measurements and estimates of the material and geometric properties of the aluminium diaphragm are presented in table 1. An external pressure is applied to the diaphragm while the single mode fibre is fixed inside the hypodermic tube using a fast-setting epoxy. The buffer (with an outside diameter of 0.25mm) remains on the fibre except in the last 2mm nearest the cleaved end. Care is required to ensure the epoxy does not contaminate the end face of fibre as this results in a loss of signal.

Symbol	Meaning	Value
ν	Poisson's ratio	0.3
E	Young's modulus	2.8 GPa
ρ	density	1955 kg/m^3
r_0	outer radius	0.15 mm
h	thickness	15 µm

Table 1. Measurements and estimates of diaphragm properties.

Calibration Shock Tube

A small shock tube was used for both the quasi-steady calibration and the dynamic calibration of the optically addressed sensor. The key dimensions of this facility are presented in figure 2. The shock tube section initially contained air from the laboratory environment at the local atmospheric pressure and ambient temperature. The laboratory ambient temperature was approximately 18°C, and the local atmospheric pressure was around 94kPa (Toowoomba is approximately 700m above sea level).

The optically addressed pressure sensor was mounted in an end-plate that was bolted to the shock tube as illustrated in figure 2. For the quasi-steady calibrations, the optically addressed sensor and mounting plate was connected directly to the driver section and the pressure within the tube was monitored with a gauge. For the dynamic calibrations, the tube configuration is illustrated in figure 2. Dynamic calibration conditions were calculated using the initial conditions within the shock tube and the incident shock speed identified using the two piezoelectric pressure transducers.

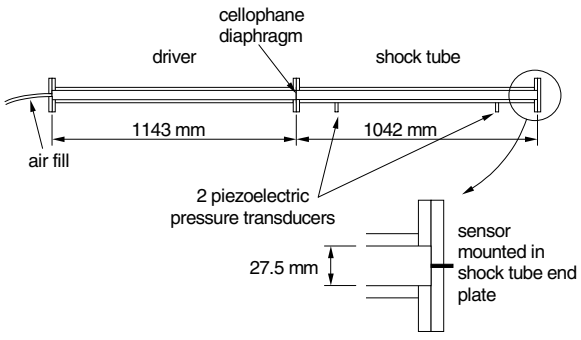

Figure 2. Calibration shock tube arrangement.

Results and Discussion

Quasi-Steady Calibration

The optical pressure transducer was calibrated by slowly increasing the pressure within the tube (over a period of about 1 hour) and recording the optical signal output (in volts) as a function of the applied pressure as illustrated in figure 3. A theoretical model for the sensitivity of the system based on the centre line deflection of a clamped diaphragm is given by [4,5],

$$\frac{\Delta\phi}{\Delta p} = \frac{4\pi n}{\lambda}\frac{3(1-\nu^2)r_0^4}{16Eh^3} \qquad (1)$$

where the symbols additional to those already defined in table 1 are:

ϕ = phase of the reflected signal
p = pressure applied to the diaphragm
n = refractive index of the cavity (≈ 1 for air)
λ = illumination wavelength (780nm)

Applying the relevant diaphragm property values (from Sensor Construction) in equation (1) gives an estimated sensitivity of 0.145rad/kPa for this sensor. Figure 3 indicates that the difference between two consecutive peaks (corresponding to a phase change of 2π radians) is about 60kPa. Thus the measured sensitivity is around 2π/60 or 0.10rad/kPa – slightly lower than the predicted value. Equation (1) is based on the centre deflection of a diaphragm with no pretension, and is thus expected to provide an upper estimate for the sensitivity of the present diaphragm arrangement.

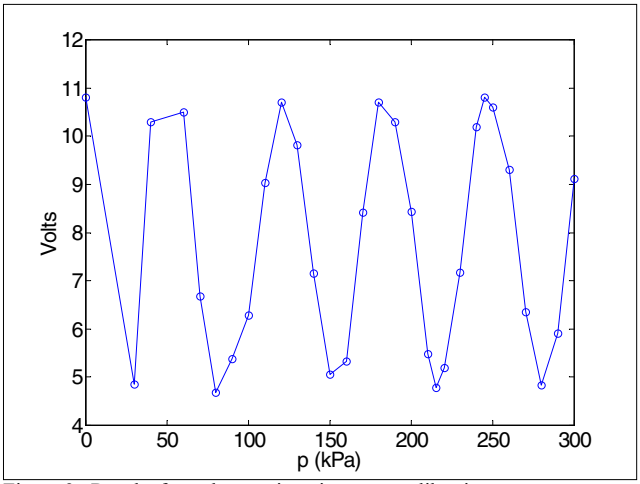

Figure 3. Results from the quasi-static sensor calibration.

Dynamic Calibration

The shock tube was operated with an air driver pressure of approximately 300kPa (absolute). Voltages from the piezoelectric pressure transducers and optically addressed sensor were recorded at 2.5Msamples/s on a Tektronix TDS420A oscilloscope. Using nominal sensitivities for the piezoelectric transducers, pressures indicated by the piezoelectric devices are presented in figure 4.

From figure 4, the shock wave time-of-flight between the first and second transducers was identified as 1.593ms. The spatial separation of the transducers was 693.5mm and thus the shock speed was 435m/s in this case. Using this shock speed and the initial pressure and temperature of the air in the shock tube (94kPa, 291K), the pressure and temperature behind the reflected shock were calculated as 268kPa and 396K respectively using the perfect gas shock wave relationships [1].

The reflected shock pressure indicated by the piezoelectric devices is around 214kPa (absolute) which is about 20% lower than the predicted value (268kPa) based on the shock speed. The cause of this difference has not yet been identified, but one possible source of error is in the sensitivity of the piezoelectric pressure transducers as an in-situ calibration of these transducers was not performed.

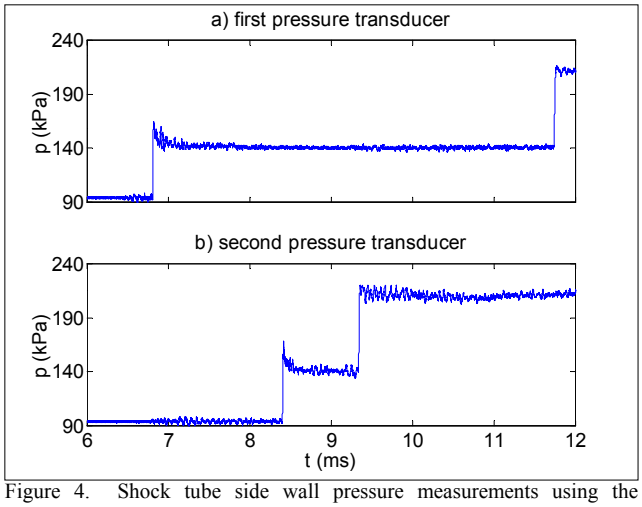

Figure 4. Shock tube side wall pressure measurements using the piezoelectric devices.

The output from the optically addressed pressure sensor subjected to shock loading over the same time scale used in figure 4 is presented in figure 5. The sensor response over 20μs immediately following shock reflection is presented in figure 6. A dominant frequency of around 300kHz can be observed in this signal toward the end of the segment illustrated in figure 6.

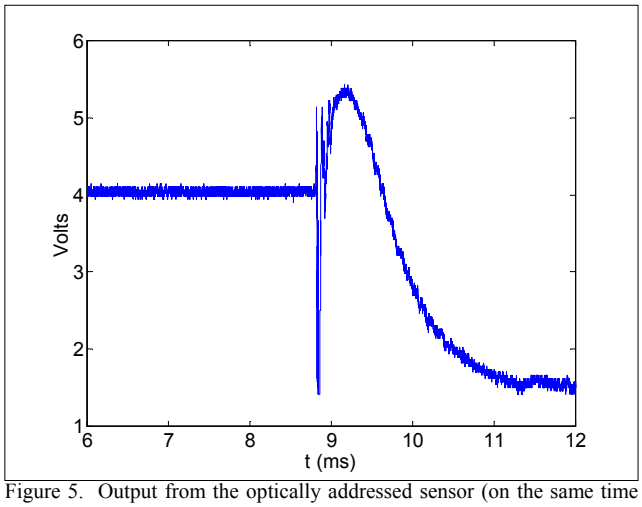

Figure 5. Output from the optically addressed sensor (on the same time scale as figure 4).

The fundamental natural frequency for a clamped circular diaphragm is given by [2]

$$f_n = \frac{10.21}{2\pi r_0^2}\sqrt{\frac{D}{h\rho}} \qquad (2)$$

where

$$D = \frac{Eh^3}{12(1-\nu^2)} \qquad (3)$$

Based on equation (2) and diaphragm properties described previously (in Sensor Construction), the fundamental natural frequency of the diaphragm is calculated as 395kHz. This is higher than the observed value of around 300kHz. Possible reasons for this difference include: 1) the effective clamped radius of the diaphragm is larger than 0.15mm (the estimated value given in Table 1); 2) the temperature of the diaphragm increases sharply immediately after shock reflection (see below for further discussion of temperature effects) and this reduces the value of Young's modulus; and 3) uncertainties in the other diaphragm properties.

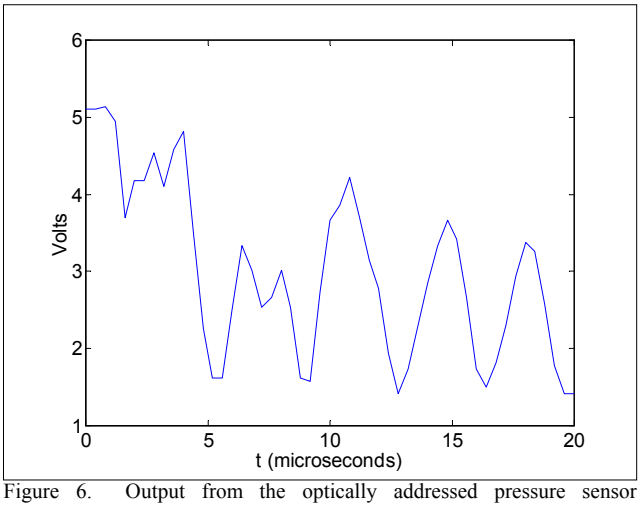

Figure 6. Output from the optically addressed pressure sensor immediately after shock reflection. (t=0 on this scale corresponds to 8.822ms on the scales in figures 4 and 5.)

The pressure behind the reflected shock is expected to be constant for a number of milliseconds – until the arrival of compression waves from the driver gas interface and the reflected expansion fan from the upstream end of the driver tube. Figure 4 confirms that the reflected shock pressure in the vicinity of the optical pressure sensor was essentially constant for at least 3ms following shock reflection from the shock tube end plate. However, the optical sensor indicates a change in cavity length during this period of essentially constant reflected shock pressure.

The reflected shock temperature was almost 400K and during the few millisecond following shock reflection it is possible that heat transfer to the diaphragm caused a substantial increase in diaphragm temperature. Aluminium has a relatively high coefficient of thermal expansion, and estimates based on the current sensor design indicate that a temperature change of only a few digress would be sufficient to account for the observed phase changes following shock reflection. Thermal finite element calculations using ANSYS55 have confirmed that the diaphragm temperature reaches within 99% of its final temperature change during the first 2.5ms following shock reflection.

Various methods could be employed to reduce the thermal sensitivity of the sensor. A diaphragm material with a lower coefficient of thermal expansion could be used. Another approach would be to coat the diaphragm with a layer of thermal insulation sufficiently thick to delay the arrival of the heat by a few milliseconds. This would allow the completion of the transient experiment prior to significant changes in the diaphragm temperature.

Conclusions

A pressure sensor utilising an interferometric measurement of diaphragm deflection with an active diaphragm diameter of 0.3mm has been constructed. Calibrations indicate that the static and dynamic pressure-response characteristics of the diaphragm can be predicted with reasonable accuracy using a clamped circular diaphragm model. However, the present sensor design also has a significant temperature sensitivity. Future work will focus on the reduction of the temperature sensitivity in transient applications through improved design and construction, and the use of a layer of thermal protection on the diaphragm.

Acknowledgments
The first author wishes to acknowledge financial support from an International Postgraduate Research Scholarship.

References

[1] Anderson, J.D., Modern Compressible Flow with historical perspective, 2nd ed., McGraw Hill, 1990.
[2] Di Giovanni, M., *Flat and Corrugated Diaphragm Design Handbook*, Marcel Dekker, 1982.
[3] He, Y. & Morgan, R.G., Transition of Compressible High Enthalpy Boundary Layer Flow Over a Flat Plate, *Aeronautical Journal*, **98**, February 1994, 25-34.
[4] MacPherson et al., Miniature Fiber Optic Pressure Sensor for Turbomachinery Applications, *Rev. Sci. Instr*., **70**, 1999, 1868-1874.
[5] MacPherson et al., Blast Pressure Measurement with a High Bandwidth Fibre Optic Pressure Sensor, *Meas. Sci. Technology*, **11**, 2000, 95-102.
[6] Mudford, N.R., Stalker, R.J. & Shields, I., Hypersonic Nozzles, *Aeronautical Quarterly*, **31**, 1980, 113-131.
[7] Neely, A.J & Morgan, R.G., The Superorbital Expansion Tube concept, experiment and analysis, *Aeronautical Journal*, **98**, March 1994, 97-105.